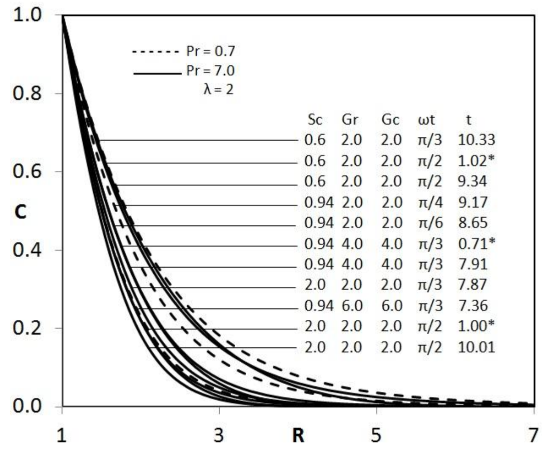

Figure 7. Transient concentration profile for different Gr, Gc and ωt.

Knowing the numerical values of velocity, temperature and concentration, the local and average skin-friction, the rate of heat transfer and mass transfer can be calculated. The local as well as average skin-friction, Nusselt number and Sherwood number in terms of dimensionless quantities are given by

$$\tau_X = -\left(\partial U / \partial R\right)_{R=1}$$

$$\bar{\tau} = -\int_0^1 \left(\partial U / \partial R\right)_{R=1} \text{ dX}$$

$$Nu_X = -X\left(\partial T / \partial R\right)_{R=1}$$

$$\overline{Nu} = -\int_0^1 \left(\partial T / \partial R\right)_{R=1} \text{ dX}$$

$$Sh_X = -X\left(\partial C / \partial R\right)_{R=1}$$

$$\overline{Sh} = -\int_0^1 \left(\partial C / \partial R\right)_{R=1} \text{ dX} \qquad (12)$$

The derivatives involved in the equations are evaluated using five-point approximation formula and then the integrals are evaluated using Newton-Cotes formula.

The local shear stress, the local heat transfer rate, and the local mass transfer rate are shown in Figs. 8–10 as functions of axial coordinate X for various values of permeability parameter, Prandtl number, and frequency parameter. The values of local skin-friction are plotted in Fig. 8. The wall shear stress is observed to increase with increasing value of X. Skin-friction increases as Pr increases since velocity gradient is more for fluids with smaller Pr (= 0.7 such as air) than for the fluids with larger Pr (= 7.0 such as water). When the permeability parameter λ increases, the value of skin friction decreases. It is seen that there is a rise in the skin-friction due to the increase in the frequency parameter ωt.

Local Nusselt number for different values of Pr, λ and ωt is shown in Fig. 9. It increases as X increases. The local heat transfer is stronger on Pr since lower Pr gives thicker temperature profiles. Larger values of Nusselt number are observed for higher value of Pr. Also, it is observed that local Nusselt number increases by the decreasing value of frequency parameter ωt. When the permeability parameter λ increases, the value of Nusselt number also increases.

The local Sherwood number is shown in Fig. 10, for various values of Pr, λ and ωt. The effect of Sc is greater on the local Sherwood number. It is observed from Fig. 6 that there is a larger concentration gradient on the cylinder. The value of Sherwood number increases as the permeability λ increases. The local mass transfer rate increases with the decrease in Prandtl number and frequency parameter ωt. This is due to the fact the concentration increases with the increase in ωt.

The average shear stress, the rate of heat transfer, and the rate of mass transfer are shown in Figs. 11–13 as functions of time for different permeability parameters, Prandtl numbers, Grashof numbers, Schmidt numbers and frequency parameter. From Fig. 11, it is observed that skin friction values increase with time and became steady after some lapse of time. Average values of skin friction get reduced with increasing values of λ throughout the transient period and also at steady-state level. The Average skin friction increases with increasing values of Pr. Moreover, initially, higher average Nusselt numbers and average Sherwood numbers are observed, and then they decrease with time.

The behaviour of average Nusselt number is similar to those described for the local Nusselt number. Figure 12 show that there is no change in Nusselt number in the initial period with respect to Pr. This reveals that heat transfer is due to conduction. The average heat transfer rate is more affected by increasing values of Pr. For the increasing values of λ, and Gr or Gc, the average Nusselt number also increases. The average heat transfer rate decreases with increasing values of ωt. Average Sherwood number or average mass transfer rate is shown in Fig. 13. It is observed that the mass transfer rate gets increased with the increase in permeability parameter λ. It decreases for increasing values of Prandtl number Pr and frequency parameter ωt.

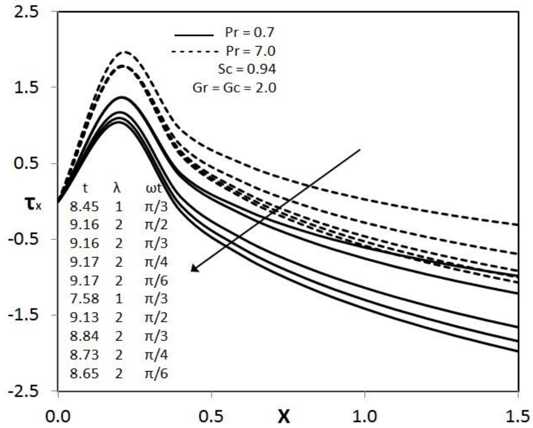

Figure 8. Local skin-friction.

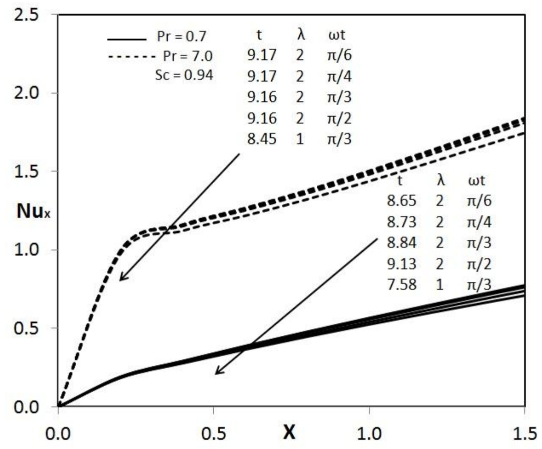

Figure 9. Local Nusselt number.

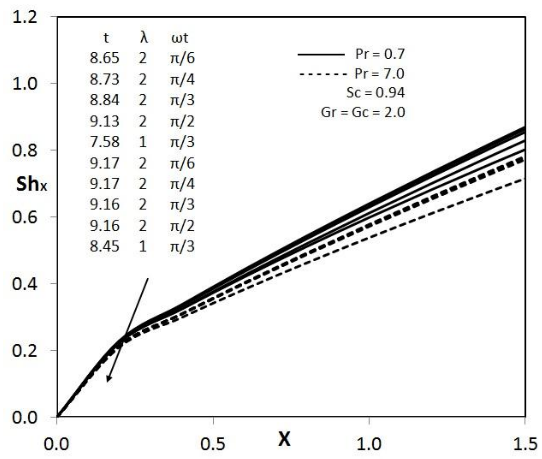

Figure 10. Local Sherwood number.

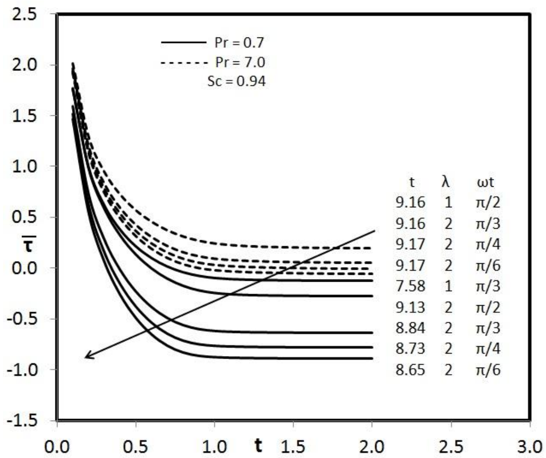

Figure 11. Average skin-friction.

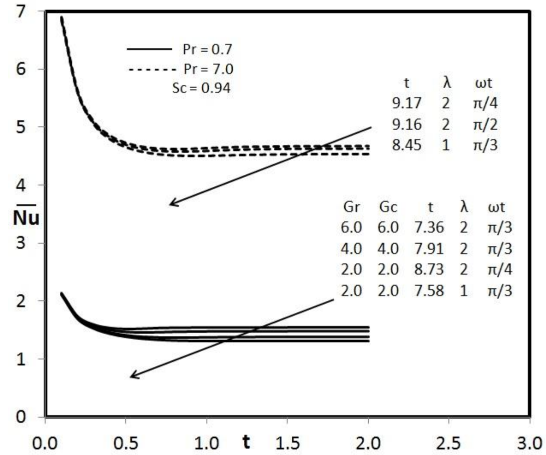

Figure 12. Average Nusselt number.

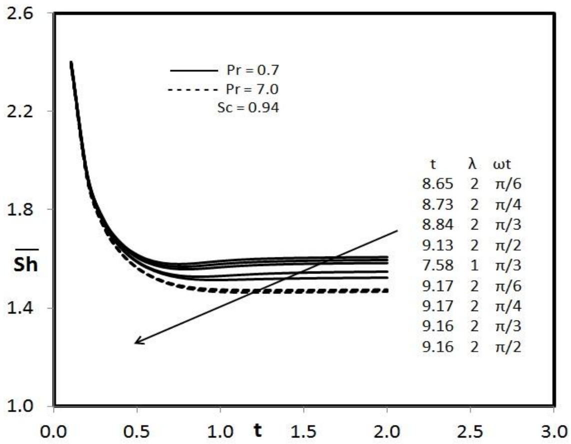

Figure 13. Average Sherwood number.

CONCLUSIONS

In this paper, the problem of natural convective flow over a moving semi-infinite vertical cylinder in the presence of porous medium along with temperature oscillation is considered. The dimensionless partial differential equations with the appropriate boundary conditions are solved numerically by an implicit finite difference method which is unconditionally stable and convergent. The effects of Prandtl number, Schmidt number, thermal Grashof number, mass Grashof number, permeability parameter and frequency parameter are shown graphically and their results are discussed. The conclusions of this study are as follows:

1. When Pr increases, there is a fall in velocity and temperature profile but there is an increase in concentration profile.
2. When λ increases, velocity and temperature profile increases but there is a decrease in concentration boundary layer.

3. When Sc increases, there is a fall in velocity and concentration profile but there is a increase in temperature profile. The time required in reaching the steady-state velocity and concentration increases with an increase in Schmidt number.
4. When ωt increases, the velocity and temperature profile decreases whereas concentration profile increases.
5. When Gr or Gc increases, there is rapid rise in the velocity profile and a fall in both temperature and concentration profiles.
6. When the permeability parameter λ increases, local heat transfer rate and local mass transfer rate increases.
7. When there is an increase in the frequency parameter, there is an increase in skin-friction and a fall in both local heat and mass rate rate.
8. Larger values of skin-friction and Nusselt number are observed for higher value of Pr and there is a fall in local Sherwood number.
9. Average values of skin friction get reduced with increasing values of λ.
10. For the increasing values of λ, and Gr or Gc, the average Nusselt number also increases. The average heat transfer rate decreases with increasing values of ωt.
11. It is observed that the mass transfer rate gets increased with the increase in permeability parameter λ. It decreases for increasing values of Prandtl number Pr and frequency parameter ωt.

REFERENCES

[1] Osvair, V. T., and Bejan, A., 1985, “Natural convection with combined heat and mass transfer buoyancy effects in a porous medium,” International Journal of Heat and Mass Transfer, 28(8), pp. 1597-1611.

[2] Soundalgekar, V. M., Lahurikar, R. M., Pohanerkar, S. G., and Birajdar, N. S., 1995, “Mass transfer effects on flow past a vertical oscillating plate with variable temperature,” Heat and Mass transfer, 30, pp. 309-312.

[3] Hossain, M. A., Das, S. K., and Pop, I., 1998, “Heat transfer response of MHD free convection flow along a vertical plate to surface temperature oscillations,” International Journal of Non-Linear Mechanics, 33(3), pp. 541-553.

[4] Ganesan, P., and Rani, H. P., 2000, “Transient natural convection flow over vertical cylinder with variable surface temperatures,” Forschung im Ingenieurwesen, 66, pp. 11-16.

[5] Li, J., Ingham, D. B., and Pop, I., 2001, “Natural convection from a vertical flat plate with a surface temperature oscillation,” International Journal of Heat and Mass Transfer, 44, pp. 2311-2322.

[6] Chen, C. H., 2004, "Heat and mass transfer in MHD flow by natural convection from a permeable, inclined surface with variable wall temperature and concentration," Acta Mechanica, 172, pp. 219-235.

[7] Saeid, N. H., 2004, "Periodic free convection from vertical plate subjected to periodic surface temperature oscillation," International Journal of Thermal Sciences, 43, pp. 569-574.

[8] Chandran, P., Sacheti, N. C., and Singh, A. K., 2005, "Natural convection near a vertical plate with ramped wall temperature," Heat Mass Transfer, 41, pp. 459-464.

[9] Ishak, A., Nazar, R., and Pop, I., 2009, "Heat transfer over an unsteady stretching permeable surface with prescribed wall temperature," Nonlinear Analysis: Real World Applications, 10, pp. 2909-2913.

[10] Chamkha, A. J., EL-Kabeir, S. M. M., and Rashad, A. M., 2011, "Heat and mass transfer by non-Darcy free convection from a vertical cylinder embedded in porous media with a temperature-dependent viscosity," International Journal of Numerical Methods for Heat & Fluid Flow, 21(7), pp. 847-863.

[11] Deka, R. K., and Paul, A., 2011, "Unsteady free convective flow past a moving vertical cylinder with constant temperature," International Journal of Mathematical Archive, 2 (6), pp. 832-840.

[12] Loganathan, P., Kannan, M., and Ganesan,P., 2011, "MHD effects on free convective flow over moving semi-infinite vertical cylinder with temperature oscillation," Applied Mathematics and Mechanics, 32(11), pp. 1367-1376.

[13] Subhashini, S. V., Sumathi, R., and Pop, I., 2013, "Dual solutions in a double-diffusive MHD mixed convection flow adjacent to a vertical plate with prescribed surface temperature," International Journal of Heat and Mass Transfer, 56, pp. 724-731.

[14] Ganesan, P., and Loganathan, P., 2001, "Unsteady free convection flow over a moving vertical cylinder with heat and mass transfer," Heat and Mass Transfer, 37(1), pp. 59-65.

[15] Carnahan, B., Luther, H. A., and Wilkes, J. O., 1969, Applied Numerical Methods, John Wiley, New York.

LIST OF SYMBOLS

Gr thermal Grashof number

g acceleration due to gravity

Nu_X local Nusselt number

$\overline{Nu}$ average Nusselt number

Sh_X	local Sherwood number
$\overline{Sh}$	average Sherwood number
Pr	Prandtl number
R	dimensionless radial co-ordinate
r	radial co-ordinate
r_0	radius of cylinder
T	temperature
t	time
U, V	dimensionless velocity components in X, R directions respectively
u, v	velocity components in x, r directions respectively
X	dimensionless axial co-ordinate

Greek symbols

α	thermal diffusivity
β	volumetric coefficient of thermal expansion
υ	kinematic viscosity
ρ	density
ω'	dimensionless frequency of oscillation
ω	frequency of oscillation
τ_X	local skin-friction
$\bar{\tau}$	average skin-friction
Δt	grid size in the time
ΔR	grid size in the radial direction
ΔX	grid size in the axial direction